

Thermal proof testing of ceramics

NOBUO KAMIYA, OSAMI KAMIGAITO

Toyota Central Research and Development Laboratories, Inc., Nagakute-cho, Aichi-gun, Aichi-ken 480-11, Japan

The possibility of thermal proof testing with thermal stress induced by quenching was examined. For this purpose, the bending strength and the critical temperature difference for quenching into water and quench oil for soda-lime-silica glass were measured before and after proof testing by quenching the specimens into water, ethyl alcohol, silicon oil and quench oil. Proof testing by water, ethyl alcohol and silicon oil quenching modified the distribution of the critical temperature difference as expected, but not that of the bending strength at all. It is suggested that proof testing by rapid quenching is a useful method for truncating the critical temperature difference distribution of ceramic components of heat engines and so on.

1. Introduction

Proof testing is one of the methods being considered as a means of improving the reliability of structural ceramic components. A number of theoretical [1-3] and experimental [4-8] studies have been carried out, which have proved that proof testing is very effective for preventing ceramics from unexpected failure in mechanical [4-7] and thermal fatigue [8]. In these studies, the proof tests have been carried out by using mechanical stresses. The use of mechanical stress as a proof stress has various advantages, for example, simplicity, ease of setting the stress, short time application of the stress and the selection of various environments. The disadvantage, however, is that it is difficult to apply a constant stress over a wide area of complicated shape components such as scrolls, combustors etc. for gas turbine engines. In contrast with mechanical stress, the thermal stress caused by quenching can be applied easily over all the surface of the component.

In the present study, to examine the possibility of proof testing by thermal stress, proof testing by quenching specimens into several liquid media was studied using a soda-lime-silica glass.

2. Experimental procedure

2.1. Specimens

The specimens used in this study are commercially available soda-lime-silica glass rods. Their dimensions are 4 mm in diameter and 75 mm in length. The specimens were cut from long bars with a diamond wheel cutter and the edges of the specimens were rounded with No. 200 diamond abrasive.

2.2. Strength measurement

Bending strength measurements were made in an atmosphere of 55% humidity at a temperature of 23°C using the three-point bending method in which the span was 40 mm. The crosshead speed was 0.5 mm min⁻¹. The initial strength distribution before proof testing was determined from 48 samples, while

that after proof testing was determined from 24 samples.

2.3. Measurement of cooling effect of quenching media

The cooling effect of the quenching media was measured by a standard method [9] with the use of a silver bar. In the measurement, a hot silver bar (diameter 10 mm, length 30 mm, 450°C) was quenched into quenching media (water, ethyl alcohol, silicon oil and quench oil) of temperature 25°C, and the surface temperature of the test bar was recorded as a function of time with a thermocouple (silver-alumel) attached to the bar, as shown in Fig. 1.

The properties of the quenching media are listed in Table I.

2.4. Thermal shock testing

In thermal shock testing, 12 specimens were vertically set in a specimen holder and then simultaneously quenched into a liquid medium after keeping them in a furnace for 30 min. The quenching media used were water, ethyl alcohol, silicon oil, and quench oil for metal as shown in Table I. The temperature of the quenching medium was controlled to be within $20 \pm 1^\circ\text{C}$. The time for transferring from the furnace to the quenching medium was about 0.4 sec. Both ends of each specimen were covered with glass fibre tube of 8 mm length to prevent the failure initiating there.

The thermal shock severity, ΔT , was the difference between the temperature of the furnace and that of the quenching medium (20°C). The temperature difference at which a specimen failed was defined as the critical temperature difference, ΔT_c . In determining the distributions of the critical temperature difference, the first thermal shock test was carried out at a lower temperature difference than ΔT_c . After confirming the non-presence of visible cracks in the specimens, each succeeding thermal shock test was carried out at a temperature difference higher by 10 or 20°C than that

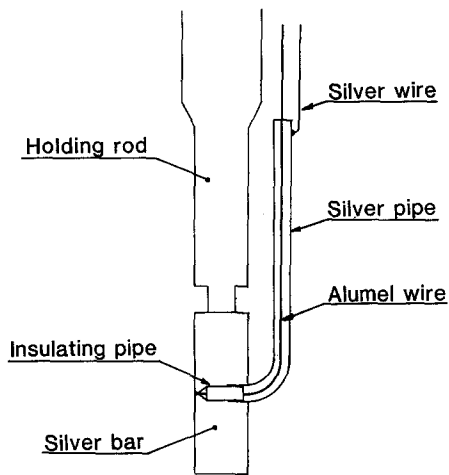


Figure 1 Schematic diagram of silver bar for measurement of cooling effect of quenching media.

in the former test, in steps. This cycle was repeated until all specimens failed. The distribution of initial critical temperature differences and those after the proof tests were determined from 24 or 48 samples.

2.5. Proof testing by quenching

Proof testing was carried out by giving a thermal shock through quenching the specimen into a liquid medium only once. Before the quenching, specimens were held in a furnace for 30 min. As quenching medium, water, ethyl alcohol, silicon oil and quench oil were used.

The temperature differences in thermal shock testing for proof testing were selected so as to break approximately 50% of a set of test specimens for each quenching medium. For the proof test survivors without visible cracks, measurements of bending strength and critical temperature difference for quenching into water and quench oil were made in the same way as described in Sections 2.2 and 2.4 to confirm the effectiveness of thermal proof testing by quenching.

3. Results and discussion

3.1. Bending strength and critical temperature difference before proof testing

The distribution of the fracture strength σ_f in ceramics can be expressed by the following Weibull statistics:

$$\ln \ln \frac{1}{1-F} = m \ln \sigma_f + C \quad (1)$$

TABLE I Typical properties of quenching media

Medium	Density (g cm ⁻³)	Viscosity (poise)*	Specific heat (cal g ⁻¹ (°C) ⁻¹) [†]	Thermal conductivity (cal cm ⁻¹ (°C) ⁻¹ sec ⁻¹) [†]	Boiling point (°C)	Heat of vaporization (cal g ⁻¹) [†]		Remarks
						20° C	Boiling point	
Water	1.00	1.00 × 10 ⁻⁴	0.999	1.42 × 10 ⁻³	100	583	540	
Ethyl alcohol	1.59	7.48 × 10 ⁻³	0.547	4.6 × 10 ⁻⁴	78.5	229	217	Extra-pure reagent
Silicon oil	0.76	8.55 × 10 ⁻³	0.34	2.4 × 10 ⁻⁴	100.5		88.8	Shin-etsu Chemical Co. Ltd KF96L 0.65CS
Quench oil	0.86	2.01 × 10 ⁻¹	0.47	3.1 × 10 ⁻⁴	300 to 450			Idemitsu Kosan Co. Ltd Gulf Super Quench

*1 poise = 10⁻¹ Pa sec.

[†]1 cal = 4.187 J.

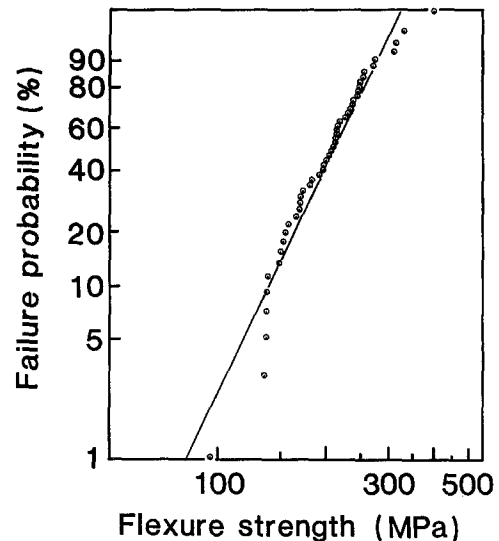


Figure 2 Weibull distribution of three-point bending strength of soda-lime-silica glass.

where F , m and C stand respectively for cumulative failure probability, Weibull modulus, and a constant.

The Weibull distribution of initial bending strength is shown in Fig. 2. The linear line in the figure was obtained by linear regression analysis. Although some experimental results deviate slightly from the straight line in the low strength region, the results agree well with the line. The Weibull modulus m determined from the straight line is 4.5. The mean value and the standard deviation of the strength are 208 and 58 MPa, respectively.

The transient thermal stress σ_T is given by the following general relations [10-12]:

$$\sigma_T = \frac{E\alpha(T_1 - T_0)}{1 - \mu} f(\beta) = \frac{E\alpha\Delta T}{1 - \mu} f(\beta) \quad (2)$$

where E is Young's modulus, α the linear coefficient of thermal expansion, μ Poisson's ratio, T_1 the initial temperature of the specimen, T_0 the temperature of the quenching medium, $f(\beta)$ a function depending on Biot's modulus β , and ΔT the temperature difference ($= T_1 - T_0$).

On the assumption that the critical temperature difference ΔT_c corresponds to the temperature difference at which a visible crack is observed in the specimen, substitution of Equation 2 into Equation 1 give

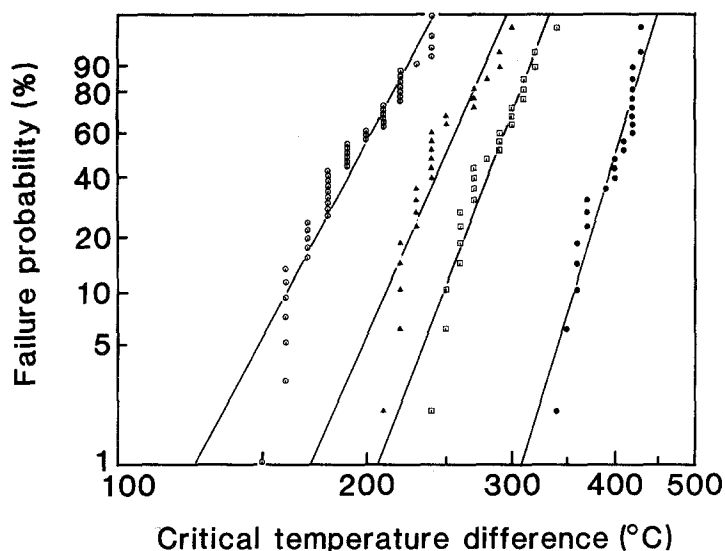


Figure 3 Weibull distribution of critical temperature difference of soda-lime-silica glass for various quenching media: (○) water, (△) ethyl alcohol, (□) silicon oil, (●) quench oil.

the equation

$$\ln \ln \frac{1}{1-F} = m \ln \Delta T_c + C' \quad (3)$$

where C' is a constant. Equation 3 reveals that the distribution of critical temperature difference can be expressed by Weibull statistics.

The distributions of critical temperature difference for various quenching media are given in the form of Weibull diagrams in Fig. 3. The experimental results for each quenching medium as well as the bending strength vary widely. In the figure, the straight lines were determined from linear regression analysis. Although some results deviate from the straight lines in the low critical temperature difference region, the results agree well with the lines, which shows that the distribution of critical temperature difference can be expressed well by Weibull statistics. As seen from Fig. 3, the critical temperature difference distribution curve shifts from a low value to a high value depending on the quenching medium, in the order water, ethyl alcohol, silicon oil, quench oil. This seems to show that the cooling effect of the quenching medium decreases in the order mentioned above. The cooling effect measured, however, is in the order water > quench oil > ethyl alcohol \cong silicon oil as shown in Fig. 4, so the order of the cooling effects does not agree with that of the critical temperature differences.

This discrepancy is considered to be due to the dependence of the crack growth rate on humidity in the quenching media. The values of water concentration in the quenching media, which were measured by Karl Fisher titration, are listed in Table II. As shown in Table II, the water concentration in ethyl alcohol is forty times as much as those of the two other media. Furthermore, oxidation of silicon oil used in present study produces water at elevated temperature [13]. In the present thermal shock testing, in which a heated

glass rod was immersed into silicon oil, water was formed on the surface of the glass rod through the reaction described above. It is well known that the crack growth rate in soda-lime-silica glass increases with water concentration [14]. Therefore the reason why the critical temperature differences for silicon oil and ethyl alcohol are both lower than that for quench oil is considered to be the dependence of crack growth rate on the water concentration in the quenching medium.

The mean values and standard deviations of the critical temperature difference and Weibull modulus for various quenching media are listed in Table III, together with the values determined from the bending strength. The Weibull moduli determined from the critical temperature difference distributions range from 9.2 to 16.3 and are considerably higher than that determined from the bending strength. Similar discrepancies between the Weibull moduli determined from bending strength and those from thermal fatigue lives of glass, Y_2O_3 -stabilized zirconia [15, 16] and sintered mullite [17] have been reported by the present authors. Although the reason for the large Weibull moduli given by thermal fatigue lives and the present critical temperature differences has not been made clear

TABLE II Water concentrations in quenching media

Quenching medium	Water concentration (p.p.m.)
Ethyl alcohol	9100
Silicon oil	160
Quench oil	250

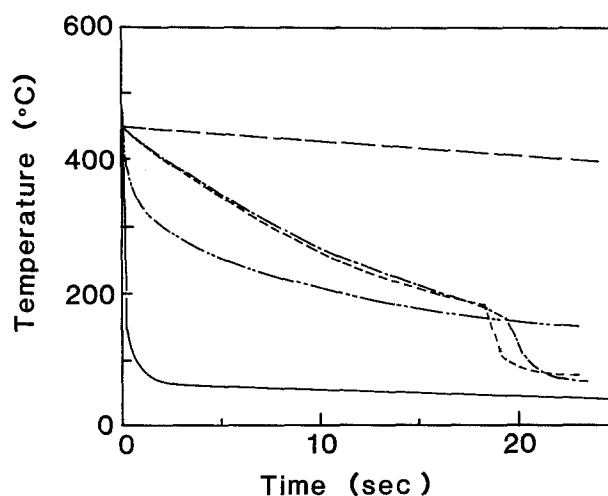


Figure 4 Cooling effect of quenching media: (---) air, (—) water, (- - -) ethyl alcohol, (---) silicon oil, (---) quench oil.

TABLE III Characteristic values of the distributions of critical temperature difference and three-point bending strength of soda-lime-silica glass

Test	Quenching medium	Critical temperature difference (°C)			Three-point bending strength (MPa)		
		Average	Standard deviation	Weibull modulus	Average	Standard deviation	Weibull modulus
Thermal shock	Water	194	25	9.2			
	Ethyl alcohol	245	26	11.3			
	Silicon oil	284	26	12.9			
	Quench oil	396	28	16.3			
Three-point bending					208	58	4.5

experimentally, it is considered to be possibly attributable to the difference of effective surface area.

Fracture modes in thermal shock testing were grouped into three modes which consist of (I) a single spiral crack, (II) a single longitudinal crack, (III) reticulated cracks as shown in Fig. 5. The fracture mode depended on the critical temperature difference. As the critical temperature difference increased the fracture mode changed from Modes I and II to Mode III, which agrees with the results of thermal shock tests on Al₂O₃ carried out by Davidge and Tappin [18] and Glandus and Boch [19].

The populations of specimens which belong to each of the classified fracture modes are listed in Table IV for each quenching medium. Thermal shock testing with quench oil gave a slightly higher value in Mode II fracture than with the other quenching media, and that with silicon oil gave a higher value in Mode III fracture. These population differences among the quenching media are considered to result from differences in the time-dependence of thermal stress at the surface of the specimen, and difference among tangential stress and axial stress.

From observation of fractured surfaces, a fracture origin in Mode I fracture was found on the surface of the fractured normal plane. Therefore, it is confirmed that in Mode I fracture, a crack initially grows normal to the specimen axis originating from a flaw which is sensitive to the normal stress, and then turns to longitudinal directions. In Mode II fracture, although the fracture origin was not found in some specimens, it is considered that a crack grows parallel to the axis from an initial flaw at the surface of the specimen which will be sensitive to tangential stress.

The fractured surfaces and the fracture origins of the specimens broken in thermal shock testing and strength testing are shown in Fig. 6. The fractured surfaces caused in strength testing consist of mirror, mist and hackle except for the specimens which failed at lower loads, which have a large area of mirror and a smaller one of hackle than those which failed at

higher loads. The surfaces broken at low load resemble those failed in thermal shock testing as shown in Fig. 6. These differences of the features among fractured surfaces are considered to be attributed to differences of crack velocity as mentioned in a previous paper [17]. The flaws acting as fracture origins seem to be caused by a contact stress during manufacturing and transportation. From observations of the flaws, the dimensions are estimated to be 50 to 210 μm in depth and 70 to 500 μm in width for the specimens which failed in thermal shock testing, and are 7 to 128 μm in depth and 17 to 342 μm in width for those in strength testing.

Thus the initial flaw size in a specimen broken by thermal shock is much larger than that in a specimen broken in strength testing. These differences among flaw distributions are thought to be attributable to differences in stressed area, since the stressed area in thermal shock testing is much larger than that in the strength testing.

3.2. Proof testing by quenching for the failure caused by thermal shock

The distributions of critical temperature difference determined by water quenching before and after proof testing, in which the quenching method is used, are given in Fig. 7. If no crack growth occurs during the proof test for the proof test survivors, the cumulative failure probability after proof testing, F_a , is described as follows [2]:

$$F_a = \frac{F - F_p}{1 - F_p} \quad (4)$$

where F is the cumulative failure probability before proof testing and F_p is that in the proof testing. In Fig. 7, the predicted lines given by Equation 4 are also drawn. The experimental results from proof test survivors by water quenching as well as ethyl alcohol quenching agree well with the predicted lines. This result suggests that the proof tests by water and ethyl alcohol quenching are very useful against thermal shock. The distribution of proof test survivors by

TABLE IV Proportions of three types of fracture mode in thermal shock testing

Medium	Fracture mode (%)		
	(I) Single spiral crack	(II) Single longitudinal crack	(III) Reticulated cracks
Water	73	8	19
Ethyl alcohol	54	8	38
Silicon oil	25	4	71
Quench oil	46	37	17

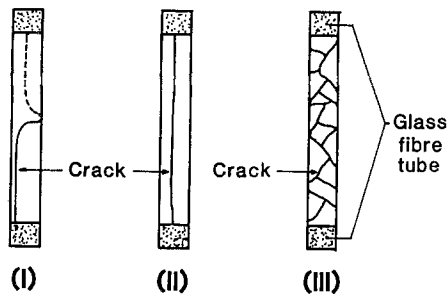


Figure 5 Fracture modes of soda-lime-silica glass in thermal shock testing: (I) spiral, (II) longitudinal, (III) reticulated. Both the solid and dotted lines indicate cracks.

silicon oil quenching does not agree with the predicted one, but some effectiveness in truncating the distribution is recognized. Moreover, the distribution of the critical temperature difference after quench-oil quenching does not agree with the predicted one, and it is rather similar to the initial distribution. From this, it is concluded that proof testing by oil quenching is not useful for the testing of failure through thermal shock. Disagreement between the proof test survivor distribution and the predicted one is considered to be attributable to crack growth during the unloading of thermal stress, as pointed out by Evans and Fuller [2] and Ritter *et al.* [6].

Therefore, the proof tests by quenching in various media become less useful in the order ethyl alcohol, water, silicon oil, quench oil. The reason is considered to be as follows: the thermal stress at the surface of the specimen caused by quenching increases up to the maximum value and then decreases with time. Evans and Fuller [2] indicated theoretically that effective proof testing can be achieved by applying rapid unloading in the test and good environmental control during the proof test. The validity of this theoretical analysis has been proved experimentally by the study of soda-lime-silica glass by Ritter *et al.* [6]. For thermal proof testing by quenching, the proof testing by quench-oil quenching was less effective than that by other quenching media. The average critical temperature difference in quench-oil quenching was 396°C higher than for the other quenching media. Therefore, it is estimated that the unloading time in quench-oil quenching is longer than that in other quenching media and the crack growth rate is higher because of the high temperature [20]. As a result, it is considered that the initial cracks of proof test survivors grow remarkably in the period of unloading, so that the critical temperature difference distribution after proof testing then differs from the ideal distribution.

The critical temperature difference distributions

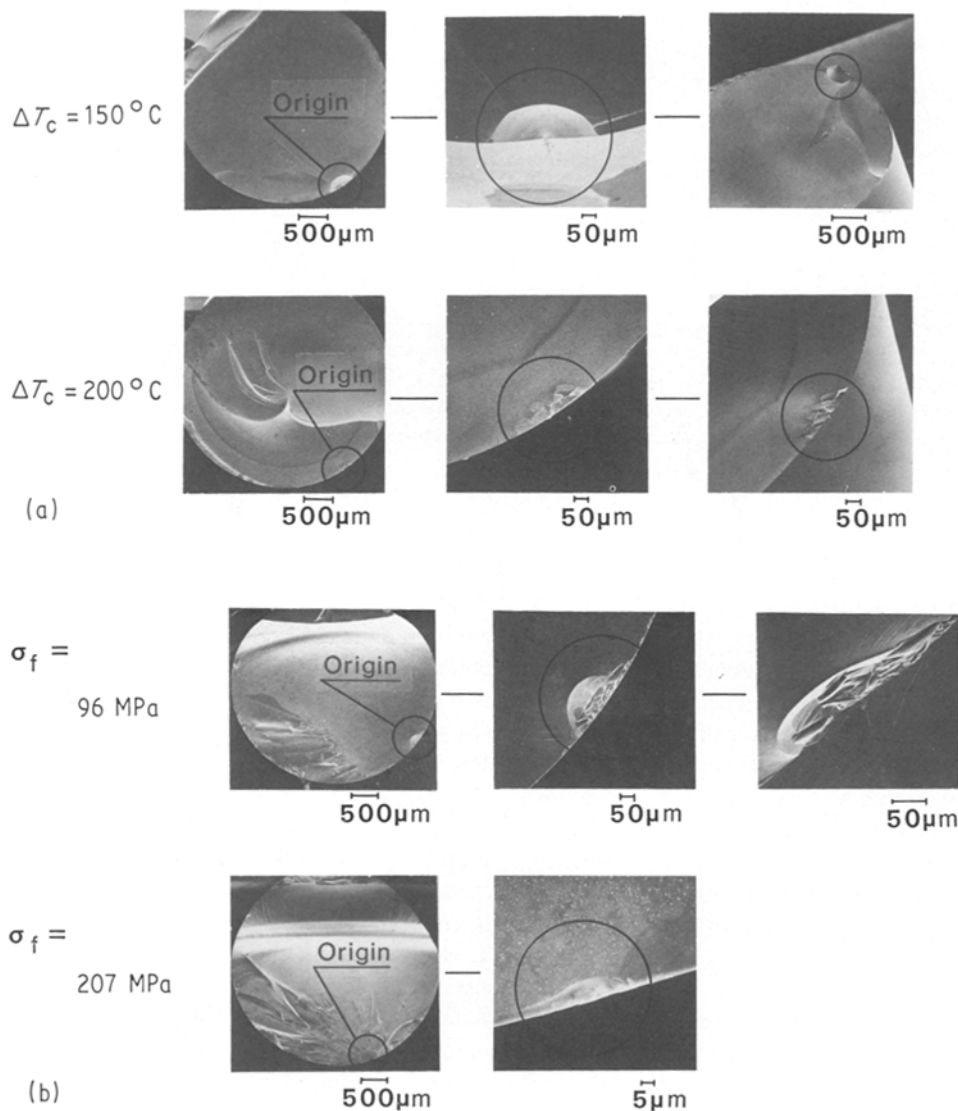


Figure 6 Typical fractured surfaces and flaws as fracture origins in (a) thermal shock testing and (b) strength testing.

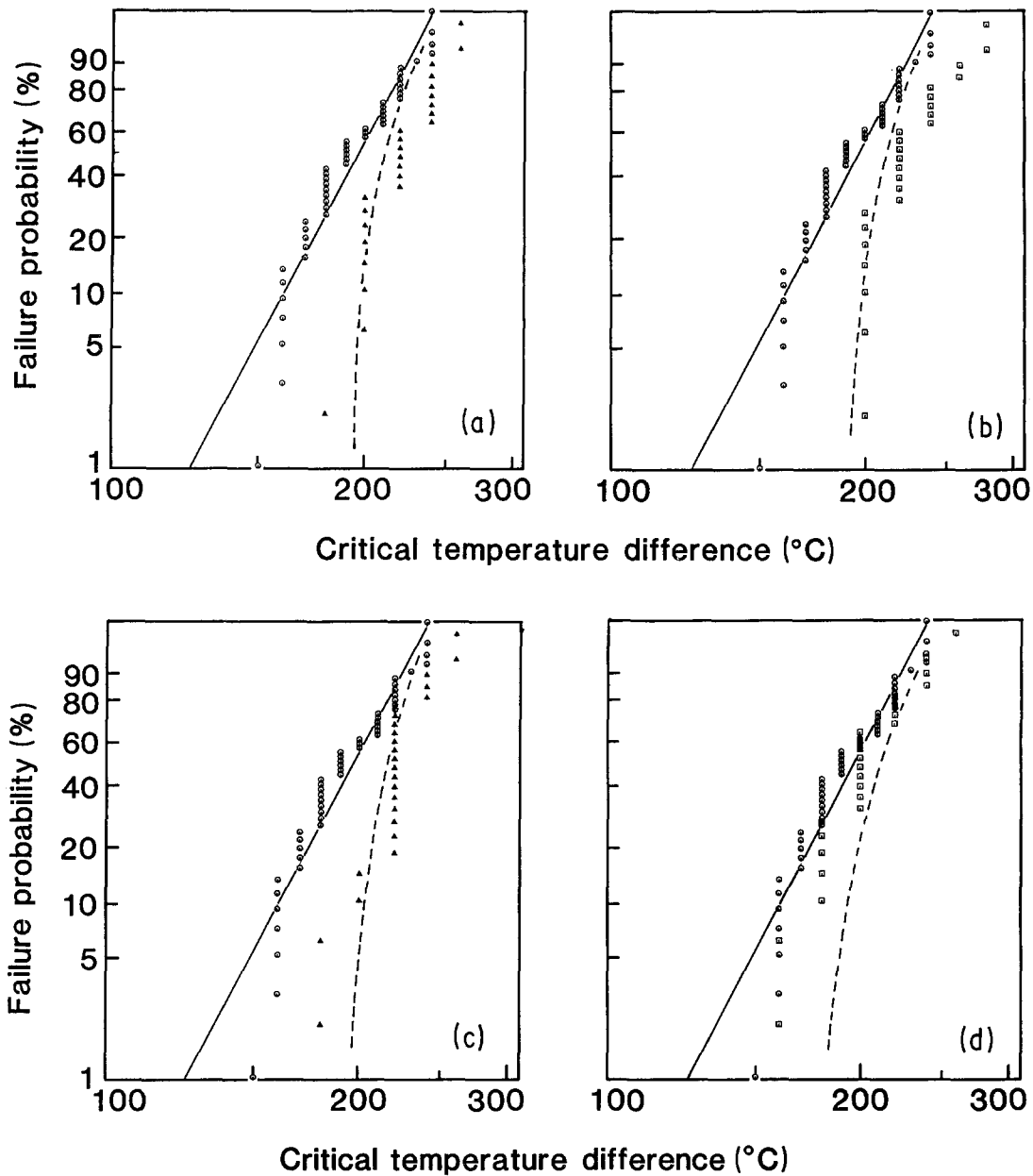


Figure 7 The effect of thermal proof testing by quenching into (a) water ($\Delta T = 190^\circ\text{C}$, $F_p = 54\%$); (b) ethyl alcohol ($\Delta T = 240^\circ\text{C}$, $F_p = 47\%$); (c) silicon oil ($\Delta T = 270^\circ\text{C}$; $F_p = 49\%$) and (d) quench oil ($\Delta T = 400^\circ\text{C}$, $F_p = 30\%$) for thermal shock by water quenching. (O) Initial distributions; (Δ , \square) after proof tests. The dashed curves show theoretical distributions of the critical temperature difference after proof testing.

determined by quench-oil quenching, in which the rate of surface temperature decrease is lower than that in water, are given in Fig. 8 for specimens before and after the proof tests in various media. The temperature difference distribution of the proof test survivors of water quenching as well as ethyl alcohol quenching agree with the predicted line in the high failure probability region, but in the low failure probability region they deviate slightly from the predicted line to a lower value, but thermal proof tests by quenching into both media are effective. Disagreements of the results with the predicted line are considered to be probably due to (i) slow crack growth during proof testing, and (ii) the difference of the type of flaw acting as the fracture origin among quench-oil, water and ethyl alcohol quenching. The first reason, however, can be denied because the decreased critical temperature difference, which must be the result of crack growth, did not occur in the thermal shock testing by water quenching

as shown in Fig. 7. On the other hand, the proportion of the fracture modes of the specimens quenched by quench-oil are different from those by water and ethyl alcohol quenching as shown in Table IV. Therefore, the disagreements are thought to be attributable to the second reason (ii) above.

Proof testing by silicon oil quenching is less useful than by water and ethyl alcohol quenching in the same way as for thermal shock testing by water quenching. The results from proof test survivors by quench-oil quenching do not agree with the predicted distribution. Thus proof testing by quenching against thermal shock caused by quench-oil quenching is less effective in the order water, ethyl alcohol, silicon oil, quench oil.

From these results, it is concluded that proof tests by rapid quenching using suitable media such as water or ethyl alcohol are very useful for avoiding the occurrence of an unexpected failure in the specimen through a transient thermal stress. This suggests that proof

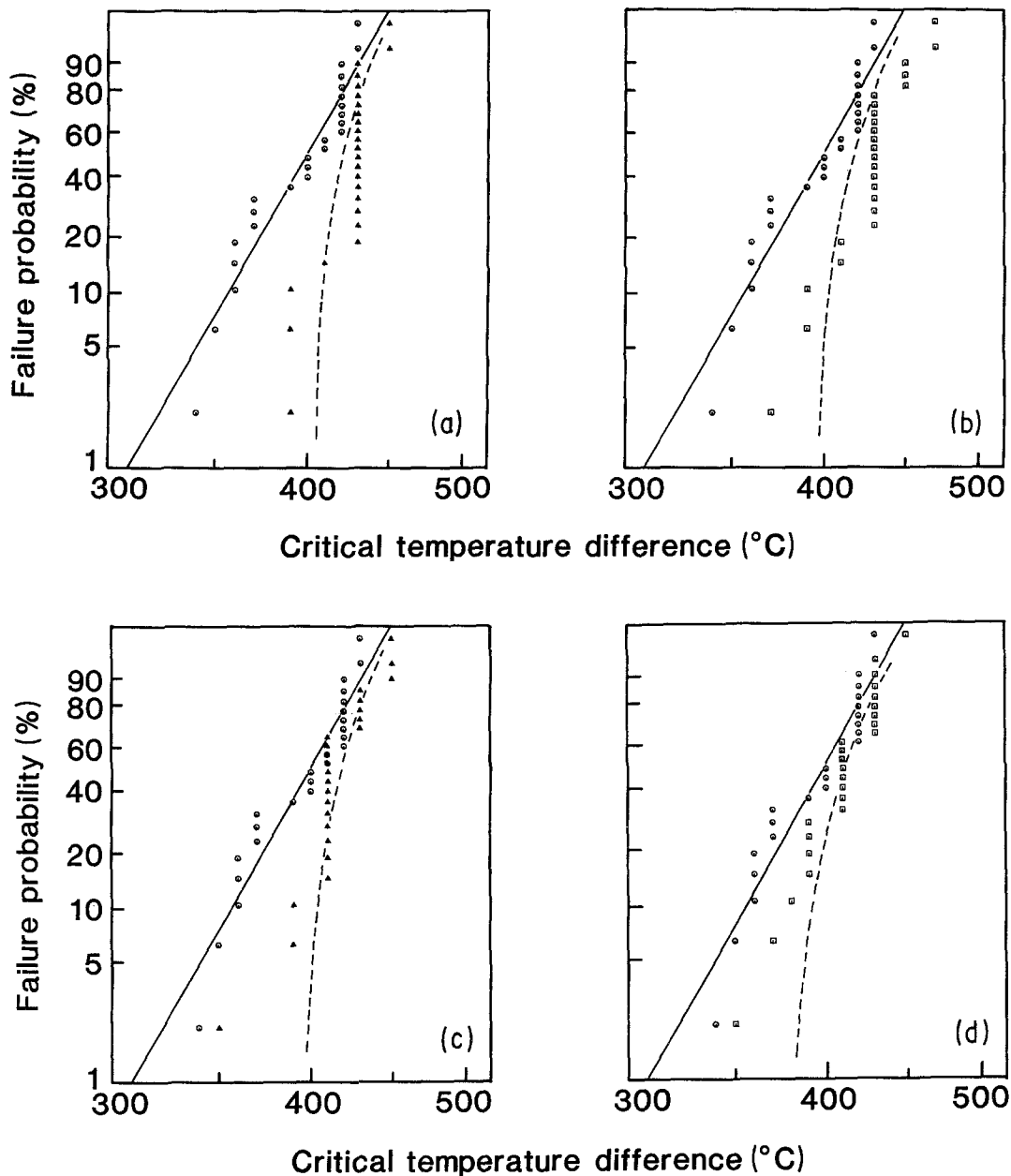


Figure 8 The effect of thermal proof testing by quenching into (a) water ($\Delta T = 190^\circ\text{C}$, $F_p = 54\%$); (b) ethyl alcohol ($\Delta T = 240^\circ\text{C}$, $F_p = 47\%$); (c) silicon oil ($\Delta T = 270^\circ\text{C}$, $F_p = 49\%$) and (d) quench oil ($\Delta T = 400^\circ\text{C}$, $F_p = 30\%$) for thermal shock by quench-oil quenching. (○) Initial distributions; (Δ , \square) after proof tests. The dashed curves show theoretical distributions of critical temperature difference after proof testing.

testing by rapid quenching would be very useful also for ceramic components in heat engines and so on.

3.3. Proof testing by quenching against the failure caused by bending stress

The bending strength distributions before and after proof testing by various quenching media are shown in Fig. 9, together with the predicted lines. Proof testing by various quenching media gave no effect on the distribution of bending strength. This lack of effect of thermal proof testing is considered to be due to the difference between the stress distribution in thermal proof testing, which is uniform over all the surface of the specimen, and that in the bending test, which varies from zero to some maximum value depending on the position in the specimen surface.

As shown in Fig. 9, the flexure strength after thermal proof testing is not smaller than the initial strength, which indicates that the initial cracks grow only slightly

on quenching. Furthermore, Badaliane *et al.* [12] calculated the crack growth of a soda-lime-silica glass rod quenched in water and indicated that the initial crack grew only slightly at a quenching temperature difference of $(\Delta T_c - 10)^\circ\text{C}$. The validity of this calculation was proved by experimental results using soda-silica-lime glass [12] and borosilicate glass [21]. Therefore, the effectiveness of thermal proof testing by quenching (Figs 7a to c, Figs 8a to c) is considered to be attributable to the occurrence of only slight crack growth.

4. Conclusions

1. Thermal proof testing by rapid quenching is effective against failure by thermal stress.
2. Water, ethyl alcohol and silicon oil are suitable as quenching media for thermal proof testing by quenching because of the possibility of rapid quenching, and the short unloading time.

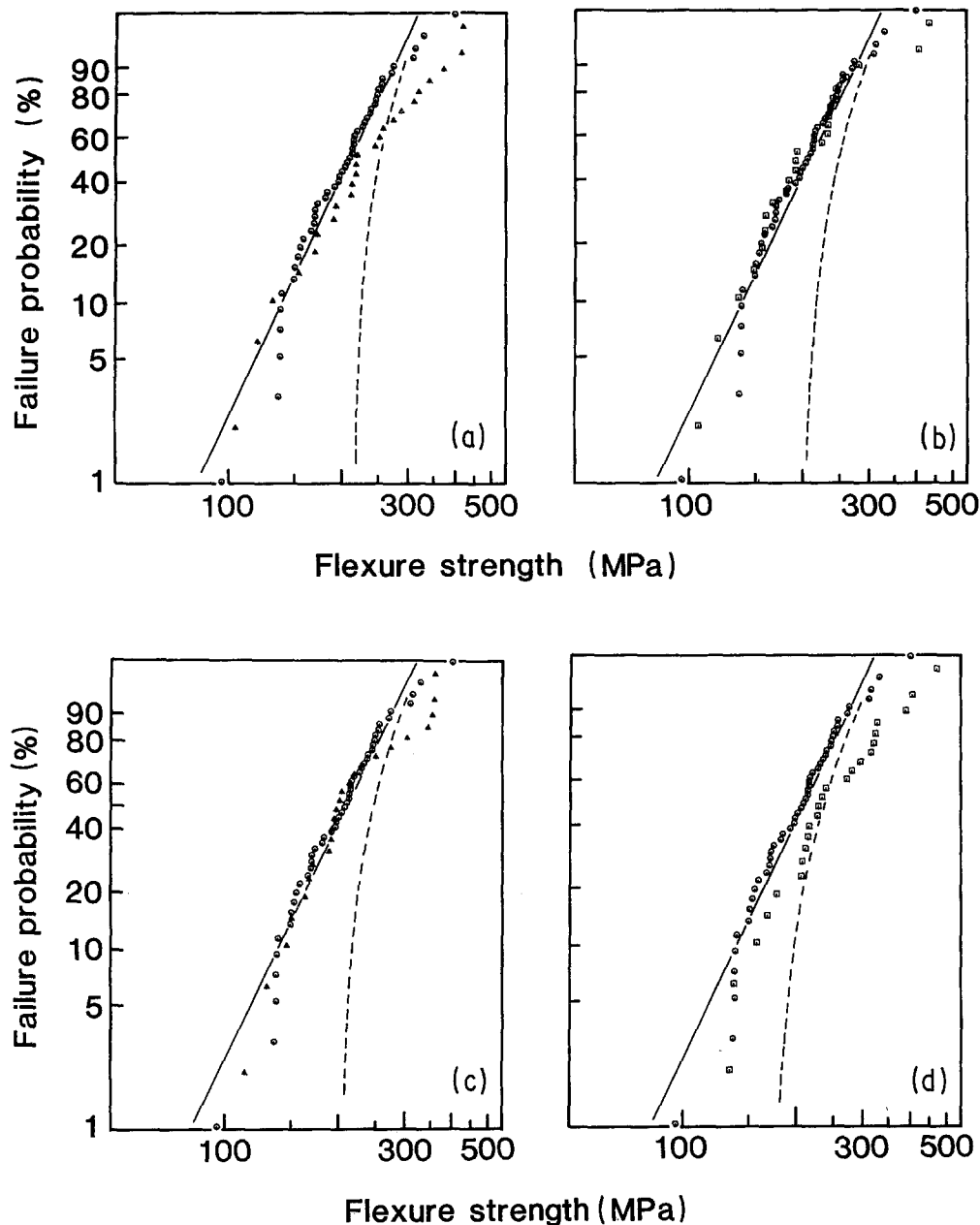


Figure 9 The effect of thermal proof testing by quenching into (a) water ($\Delta T = 190^\circ\text{C}$, $F_p = 54\%$); (b) ethyl alcohol ($\Delta T = 240^\circ\text{C}$, $F_p = 47\%$), (c) silicon oil ($\Delta T = 270^\circ\text{C}$, $F_p = 49\%$) and (d) quench oil ($\Delta T = 400^\circ\text{C}$, $F_p = 30\%$) for three-point bending strength. (O) Initial distributions; (Δ , \square) after proof tests. The dashed curves show theoretical distributions of strength after proof testing.

References

1. A. G. EVANS and S. M. WIEDERHORN, *Int. J. Fract.* **10** (1974) 379.
2. A. G. EVANS and E. R. FULLER, *Mater. Sci. Engng* **13** (1975) 69.
3. E. R. FULLER, S. M. WIEDERHORN, J. E. RITTER and P. B. OATES, *J. Mater. Sci.* **15** (1980) 2282.
4. S. M. WIEDERHORN and N. J. TIGHE, *ibid.* **19** (1978) 1781.
5. J. E. RITTER and S. A. WULF, *Amer. Ceram. Soc. Bull.* **57** (1978) 186.
6. J. E. RITTER, P. B. OATES, E. R. FULLER and S. M. WIEDERHORN, *J. Mater. Sci.* **15** (1980) 2275.
7. K. JAKUS, J. P. FAHEY and J. E. RITTER, in "Fracture Mechanics of Ceramics", Vol. 5, edited by R. C. Bradt, D. P. H. Hasselman and F. F. Lange (Plenum, New York, 1983) p. 425.
8. N. KAMIYA and O. KAMIGAITO, *J. Mater. Sci.* **16** (1981) 828.
9. JIS K2526 (Japanese Standards Association, 1965).
10. W. D. KINGERY, H. K. BOWEN and D. R. UHLMANN, "Introduction to Ceramics", 1st Edn (Wiley, New York, 1967) p. 632.
11. D. P. H. HASSELMANN, *J. Amer. Ceram. Soc.* **52** (1969) 600.
12. R. BADALIANCE, D. A. KROHN and D. P. H. HASSELMANN, *ibid.* **59** (1974) 432.
13. R. C. GUNDERSON and A. W. HART, "Synthetic Lubricants" (Chapman & Hall, London, 1962) pp. 264-319.
14. S. M. WIEDERHORN, *J. Amer. Ceram. Soc.* **50** (1967) 407.
15. N. KAMIYA and O. KAMIGAITO, *J. Mater. Sci.* **14** (1979) 573.
16. *Idem*, *ibid.* **17** (1982) 3149.
17. *Idem*, *J. Ceram. Soc. Jpn* **95** (1985) 275.
18. R. W. DAVIDGE and G. TAPPIN, *Trans. Br. Ceram. Soc.* **66** (1967) 405.
19. J. C. GLANDUS and P. BOCH, *Int. J. Thermophys.* **2** (1981) 89.
20. S. M. WIEDERHORN and L. H. BOLZ, *J. Amer. Ceram. Soc.* **53** (1970) 543.
21. M. ASHIZUKA, T. E. EASLER and R. C. BRADT, *ibid.* **66** (1983) 542.

Received 11 December 1987
and accepted 6 May 1988